

## Electronic Supplementary Information

# Mixture effect assessment applying *in vitro* bioassays to *in-tissue* silicone extracts of traditional foods prepared from beluga whale blubber

Beate I. Escher, Matthew J. Binnington, Maria König, Ying D. Lei and Frank Wania

## ESI -Tables (see attached excel workbook)

**Table S1.** Sample ID lipid uptake into PDMS and lipid uptake-adjusted distribution ratio between lipids and PDMS.

**Table S2.** Blank-corrected, recovery-corrected, and lipid-adjusted concentrations of OCPs (ng/g<sub>lipid</sub>) measured in beluga TF samples via direct blubber extraction. Reprinted with permission from Binnington, M.J., Lei, Y.D., Pokiak, L., Pokiak, J., Ostertag, S.K., Loseto, L.L., Chan, H.M., Yeung, L.W.Y., Huang, H. and Wania, F. (2017). Effects of preparation on nutrient and environmental contaminant levels in Arctic beluga whale (*Delphinapterus leucas*) traditional foods. Environmental Science-Processes & Impacts, 19(8), 1000-1015.

**Table S3.** Cytotoxicity expressed as inhibitory concentration for 10% reduction of cell viability IC<sub>10</sub> (kg<sub>PDMS</sub>/L<sub>bioassay</sub>) and toxic units TU (L<sub>bioassay</sub>/kg<sub>lipid</sub>) for all cell lines.

**Table S4.** Effect concentrations EC<sub>10</sub> (kg<sub>PDMS</sub>/L<sub>bioassay</sub>) converted to EC<sub>10</sub> (kg<sub>lipid</sub>/L<sub>bioassay</sub>)

**Table S5.** Concentrations of OCPs and PCBs in lipid (ng/g<sub>lipid</sub>) calculated from PDMS concentrations and K<sub>lip/PDMS</sub> from literature (A. Jahnke, M. S. McLachlan and P. Mayer, Equilibrium sampling: Partitioning of organochlorine compounds from lipids into polydimethylsiloxane, Chemosphere, 2008, 73, 1575-1581.)

**Table S6.** Effect concentrations of detected chemicals (Data from J. Lee, G. Braun, L. Henneberger, M. König, R. Schlichting, S. Scholz and B. I. Escher, Critical Membrane Concentration and Mass-Balance Model to Identify Baseline Cytotoxicity of Hydrophobic and Ionizable Organic Chemicals in Mammalian Cell Lines, Chem. Res. Toxicol., 2021, 34, 2100-2109.)

**Table S7.** Iceberg modelling: Bioanalytical equivalent concentrations BEQ from bioassay measurements (BEQ<sub>bio</sub>) and predicted BEQ<sub>chem</sub> from the chemical concentrations (Table S2) and their relative effect potencies (calculated from the effect concentrations in Table S6) as well as % effect explained by the detected chemicals.

## ESI Figures (this document)

**Figure S1.** Study outline.

**Figure S2.** Comparison of lipid-based toxic units, indicative of cytotoxicity, TU<sub>bio</sub> of the different samples between the two Beluga whales HI-14-11 and HI-14-06. HI-14-06 is the older of the two individuals. Data are from Table S3.

**Figure S3.** Cumulative toxic units TU<sub>bio</sub> for cytotoxicity of the different cell lines. The vertical line at log TU<sub>bio</sub> = 2.3 represents the highest concentration without detected cytotoxicity. The rank distributions at lower TU<sub>bio</sub> were extrapolated. Data are from Table S3.

**Figure S4.** Concentration-response curves (CRCs) for the PDMS Blanks in (a) AhR-CALUX, (b) PPAR γ-bla, (c) ERα-bla, (d) AR-bla, (e) GR-bla, (f) PR-bla, (g) AREc32.

**Figure S5.** Concentration-response curves for the Muktuk samples of whales HI-14-11 (left) and HI-14-06 (right) in the AhR-CALUX assay.

**Figure S6.** Concentration-response curves for the Uqsuq samples of whales HI-14-11 (left) and HI-14-06 (right) in the AhR-CALUX assay.

**Figure S7.** Concentration-response curves for the Muktuk samples of whales HI-14-11 (left) and HI-14-06 (right) in the PPARγ-bla assay.

**Figure S8.** Concentration-response curves for the Uqsuq samples of whales HI-14-11 (left) and HI-14-06 (right) in the PPARγ-bla assay.

**Figure S9.** Plot indicating that there is no association between the Rosiglitazone-EQ [ng<sub>Rosiglitazone</sub>/g<sub>lipid</sub>] (Table S7) and the weight gain due to lipid uptake (Table S1).

**Figure S10.** Concentration-response curves for the Muktuk samples of whales HI-14-11 (left) and HI-14-06 (right) in the ERα-bla assay.

**Figure S11.** Concentration-response curves for the Uqsuq samples of whales HI-14-11 (left) and HI-14-06 (right) in the ER $\alpha$ -bla assay.

**Figure S12.** Concentration-response curves for the Muktuk samples of whales HI-14-11 (left) and HI-14-06 (right) in the AR-bla assay.

**Figure S13.** Concentration-response curves for the Uqsuq samples of whales HI-14-11 (left) and HI-14-06 (right) in the AR-bla assay.

**Figure S14.** Concentration-response curves for the Muktuk samples of whales HI-14-11 (left) and HI-14-06 (right) in the GR-bla assay.

**Figure S15.** Concentration-response curves for the Uqsuq samples of whales HI-14-11 (left) and HI-14-06 (right) in the GR-bla assay.

**Figure S16.** Concentration-response curves for the Muktuk samples of whales HI-14-11 (left) and HI-14-06 (right) in the PR-bla assay.

**Figure S17.** Concentration-response curves for the Uqsuq samples of whales HI-14-11 (left) and HI-14-06 (right) in the PR-bla assay.

**Figure S18.** Concentration-response curves for the Muktuk samples of whales HI-14-11 (left) and HI-14-06 (right) in the AREc32 assay.

**Figure S19.** Concentration-response curves for the Uqsuq samples of whales HI-14-11 (left) and HI-14-06 (right) in the AREc32 assay.

**Figure S20.** Comparison of effect concentrations EC10 for the activation of reporter genes. Data in Table S4.

**Figure S21.** Comparison of concentrations of analytes in lipids from direct extraction and via PDMS extraction. Data in Table S2 and S5.

**Figure S22.** Bioassay medium-air partition constants  $K_{\text{medium/air}}$  for all detected chemicals. The dotted line is the “volatility cutoff” of  $K_{\text{medium/air}} = 10^4$  and all chemicals with lower  $K_{\text{medium/air}}$  are expected to escape during the bioassay exposure.

**Figure S23.** Comparison between the predicted baseline toxicity IC<sub>10</sub> calculated with the model of Lee et al.<sup>1</sup> and the measured cytotoxicity IC<sub>10</sub> and response concentrations for the specific effects. Only chemicals below the 1:1 line show a specific effect, most chemicals are active but merely as baseline toxicants. Data from Table S6.

**Figure 24.** Comparison between the bioanalytical equivalent concentrations predicted from the detected chemicals (BEQ<sub>chem</sub>) and the contribution to BEQ<sub>chem</sub> by (a) PAHs and (b) other chemicals in the AhR-CALUX. Data in Table S7.

**Figure 25.** Comparison between the bioanalytical equivalent concentrations as derived from the bioassays (BEQ<sub>bio</sub>) and as derived from the measured concentrations of the detected chemicals (BEQ<sub>chem</sub>) for (a) AhR-CALUX, (b) PPAR $\gamma$ -bla and (c) AREc32 Data in Table S7.

**Figure S26.** Contribution of nonpersistent polycyclic aromatic hydrocarbons (PAHs) and persistent organochlorine pesticides (OCPs) to B[a]P-EQ<sub>chem</sub> in the AREc32 assay. Data in Table S7.

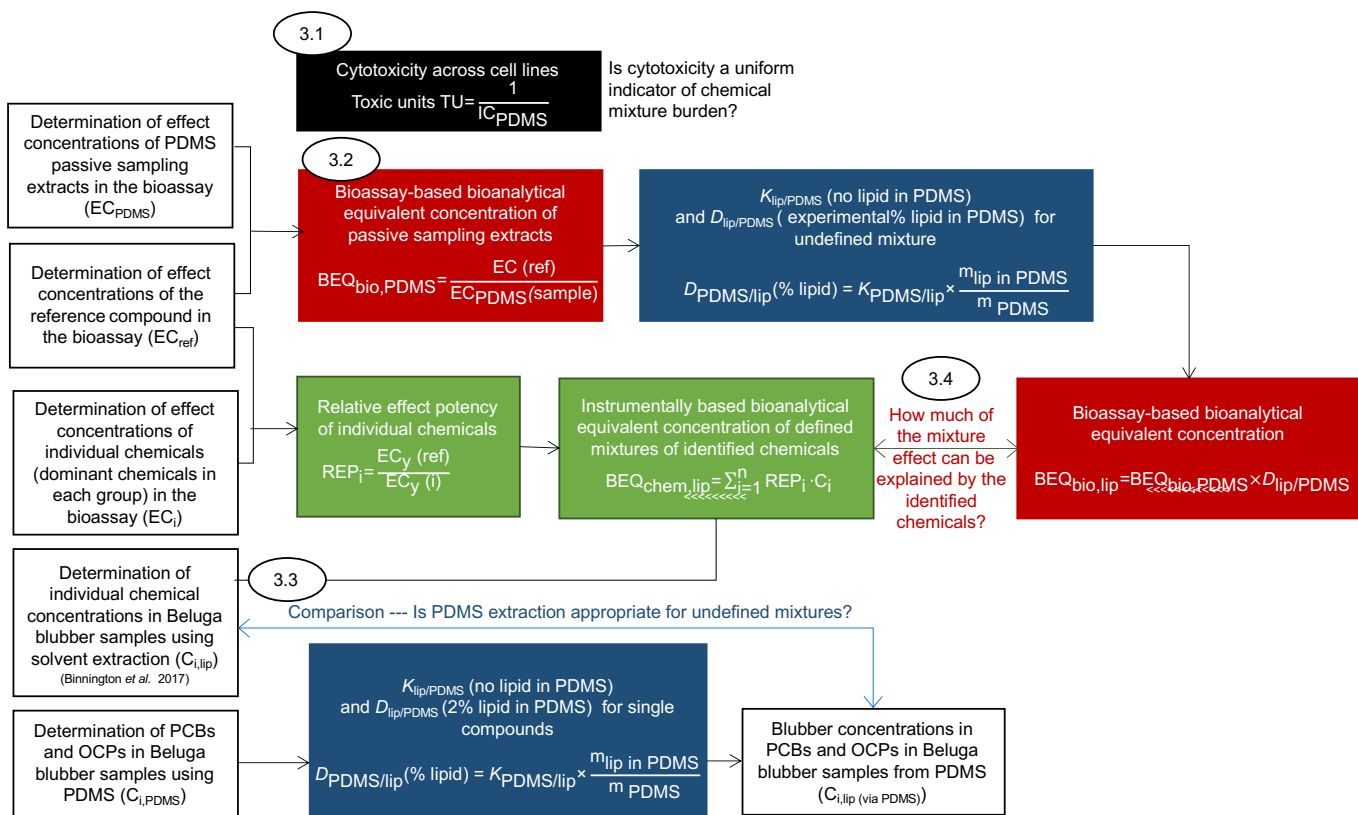


Figure S 1. Study outline. Numbers in ovals refer to sections in the main paper. The white boxes are the experimental data, the black box describe the data treatment for cytotoxicity, the red boxes the data treatment for effect data, the blue boxes convert the effect data from PDMS to lipid concentrations, the green boxes explain the calculation of predicted bioanalytical equivalent concentrations  $BEQ_{chem}$  from the chemical concentrations and their relative effect potencies. The questions not in boxes the three main questions.

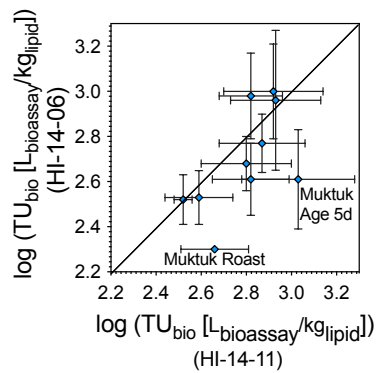


Figure S 2. Comparison of lipid-based toxic units, indicative of cytotoxicity,  $TU_{bio}$  of the different samples between the two Beluga whales HI-14-11 and HI-14-06. HI-14-06 is the older of the two individuals. Data are from Table S3.

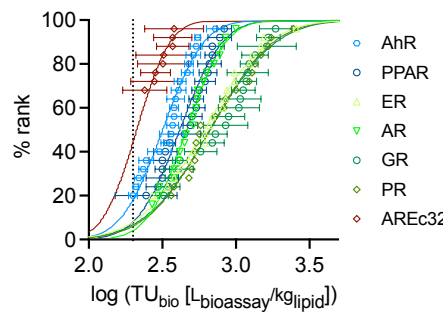


Figure S 3. Cumulative toxic units  $TU_{bio}$  for cytotoxicity of the different cell lines. The vertical line at  $\log TU_{bio} = 2.3$  represents the highest concentration without detected cytotoxicity. The rank distributions at lower  $TU_{bio}$  were extrapolated. Data are from Table S3.

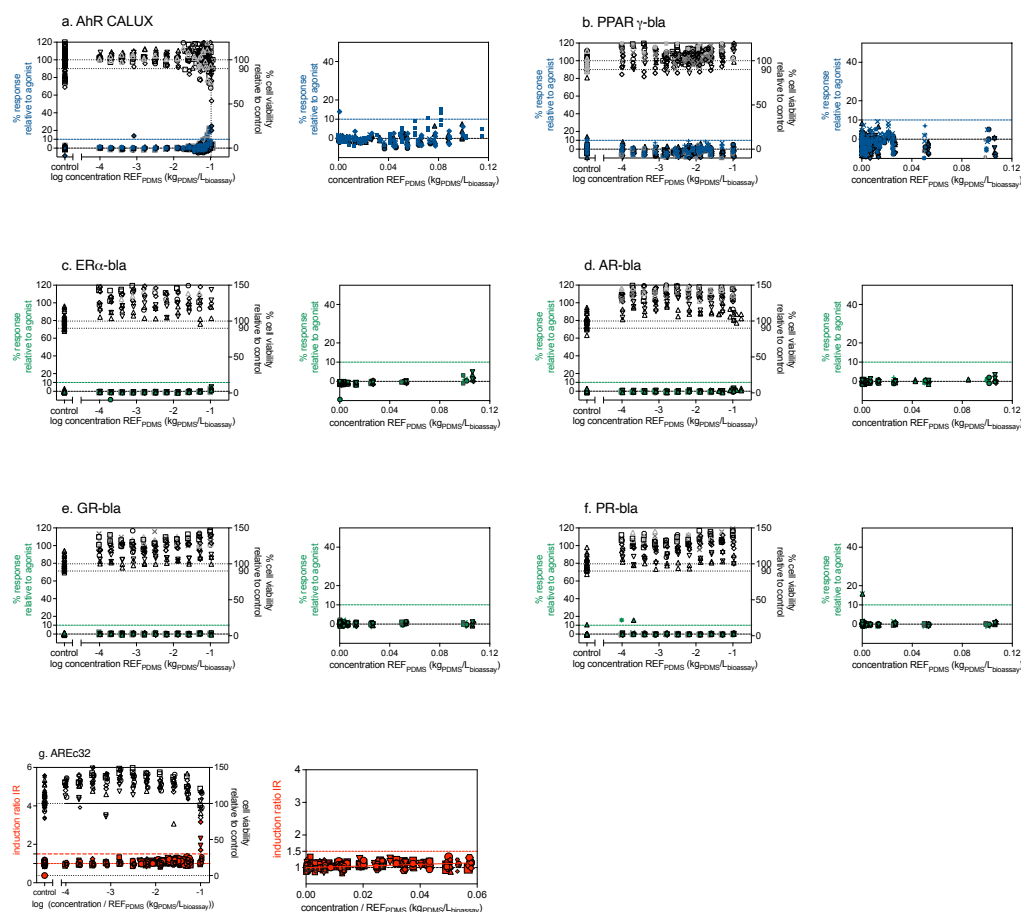


Figure S 4. Concentration-response curves (CRCs) for the PDMS Blanks in (a) AhR-CALUX, (b) PPAR  $\gamma$ -bla, (c) ER $\alpha$ -bla, (d) AR-bla, (e) GR-bla, (f) PR-bla, (g) AREc32. The left figures contain all data (cell viability and activation of the reporter gene) on a log-concentration scale, the right figures contain only the activation data up to  $IC_{10}$  concentrations on a linear scale. The dotted line in (a) corresponds to the approximate  $IC_{10}$  of  $0.1 \text{ kg}_{\text{POMS}}/\text{L}_{\text{bioassay}}$  for cytotoxicity.

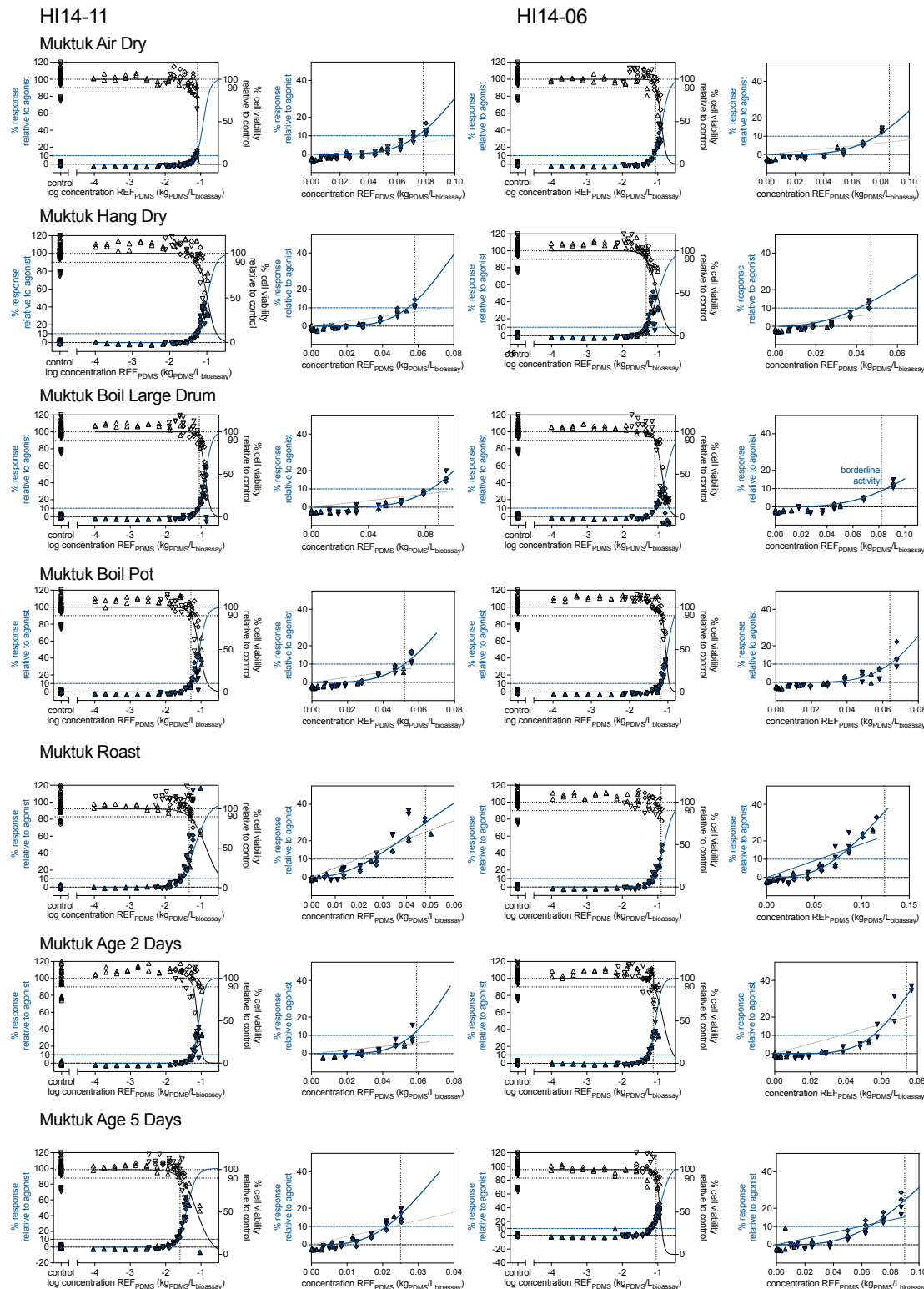


Figure S 5. Concentration-response curves for the Muktuk samples of whales HI-14-11 (left) and HI-14-06 (right) in the Ahr-CALUX assay. For each sample, the left plot is on the log-concentration scale to determine the cytotoxicity. The vertical dotted line indicates the  $IC_{10}$  for cytotoxicity. The  $EC_{10}$  was derived from the portion of the CRC up to  $IC_{10}$ . The full blue line refers to the log-sigmoidal CRC model, the thin line to the linear model, which did not yield a satisfactory fit and was not applied. The blue dotted line marks the 10% effect level.  $IC_{10}$  values are in Table S3 and  $EC_{10}$  values from the are in Table S4.

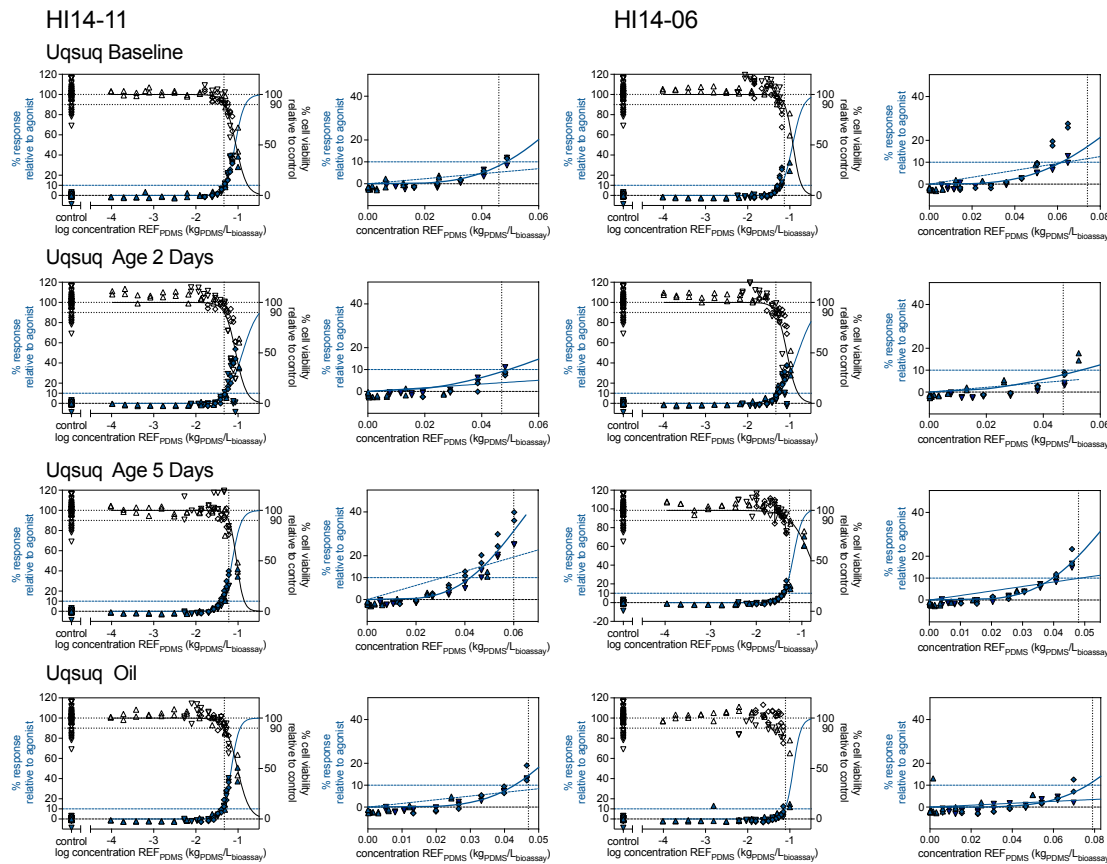


Figure S 6. Concentration-response curves for the Uqsuq samples of whales HI-14-11 (left) and HI-14-06 (right) in the AhR-CALUX assay. For each sample, the left plot is on the log-concentration scale to determine the cytotoxicity. The vertical dotted line indicates the  $IC_{10}$  for cytotoxicity. The  $EC_{10}$  was derived from the portion of the CRC up to  $IC_{10}$ . The full blue line refers to the log-sigmoidal CRC model, the thin line to the linear model, which did not yield a satisfactory fit and was not applied. The blue dotted line marks the 10% effect level.  $IC_{10}$  values are in Table S3 and  $EC_{10}$  values from the are in Table S4.

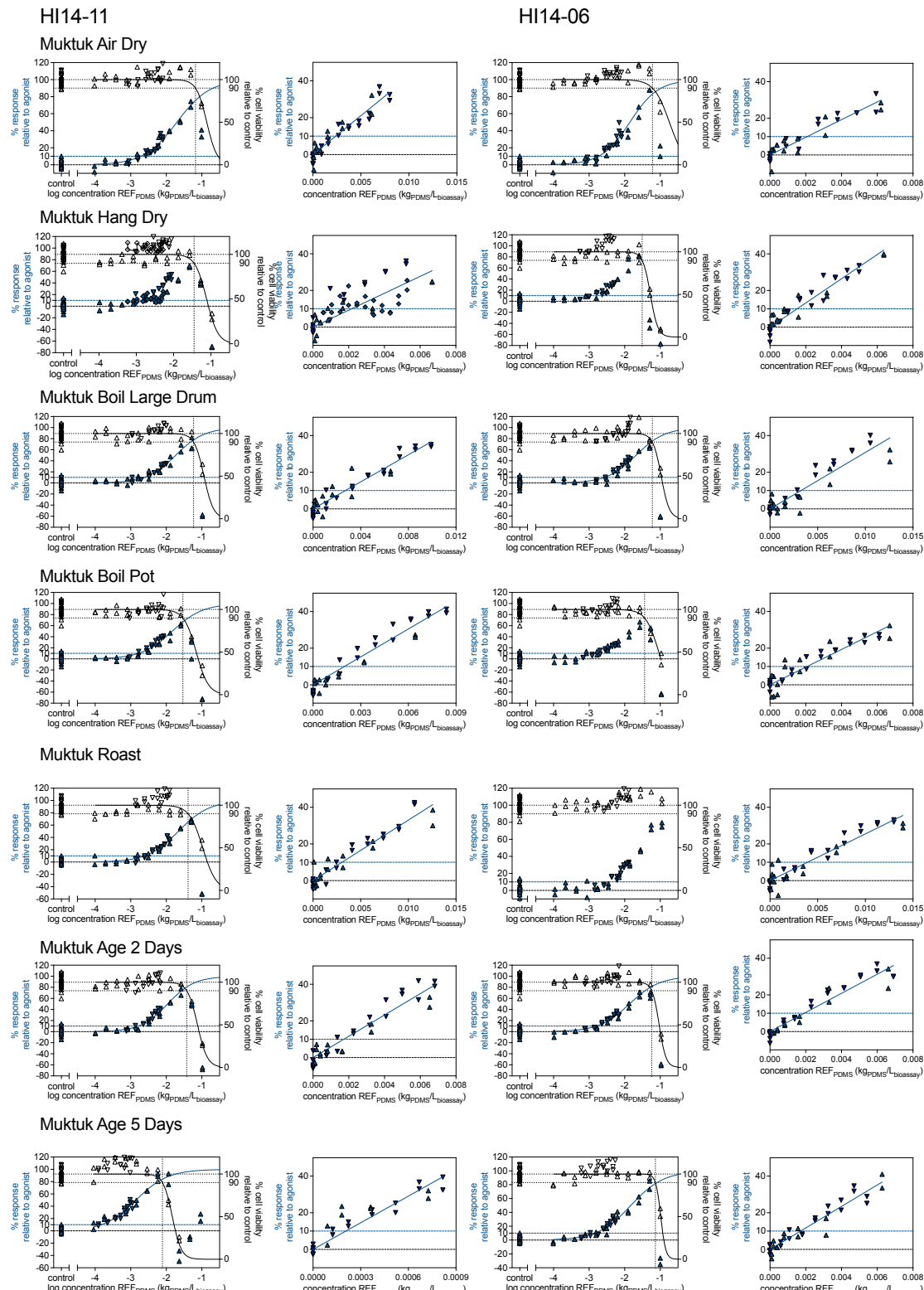


Figure S 7. Concentration-response curves for the Muktuk samples of whales HI-14-11 (left) and HI-14-06 (right) in the PPAR $\gamma$ -bla assay. For each sample, the left plot is on the log-concentration scale to determine the cytotoxicity. The vertical dotted line indicates the IC<sub>10</sub> for cytotoxicity. All % effect values above IC<sub>10</sub> concentrations or above 40% effect were excluded for the linear concentration effect curves in each of the right plots. The EC<sub>10</sub> was derived from the linear regression of the concentration versus IR. The blue dotted line marks the 10% effect level. IC<sub>10</sub> values are in Table S3 and EC<sub>10</sub> values from the are in Table S4.

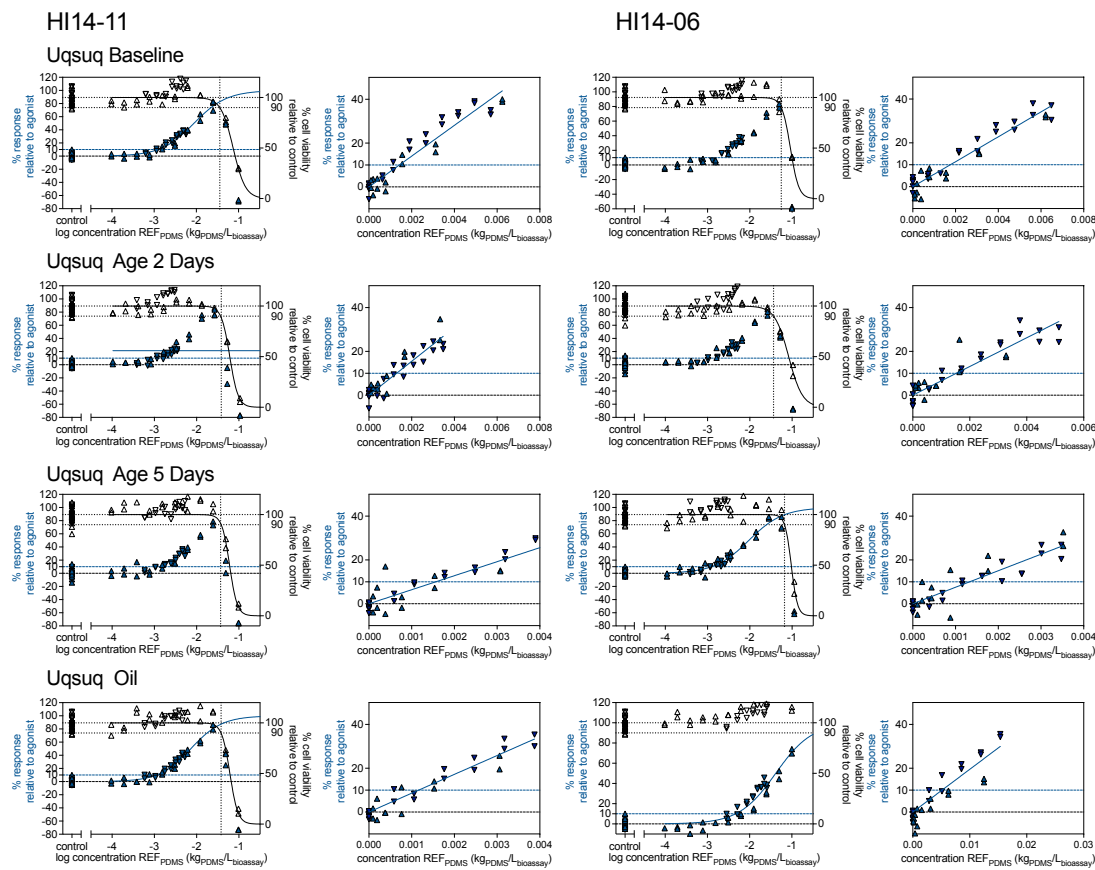


Figure S 8. Concentration-response curves for the Uqsuq samples of whales HI-14-11 (left) and HI-14-06 (right) in the PPAR $\gamma$ -bla assay. For each sample, the left plot is on the log-concentration scale to determine the cytotoxicity. The vertical dotted line indicates the IC<sub>10</sub> for cytotoxicity. All % effect values above IC<sub>10</sub> concentrations or above 40% effect were excluded for the linear concentration effect curves in each of the right plots. The EC<sub>10</sub> was derived from the linear regression of the concentration versus IR. The blue dotted line marks the 10% effect level. IC<sub>10</sub> values are in Table S3 and EC<sub>10</sub> values from the are in Table S4.

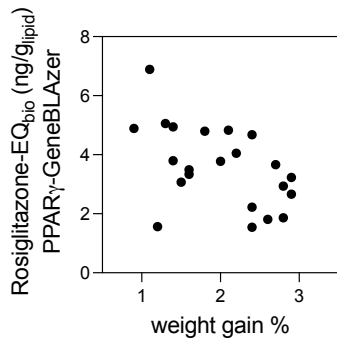


Figure S 9. Plot indicating that there is no association between the Rosiglitazone-EQ [ng<sub>Rosiglitazone</sub>/g<sub>Lipid</sub>] (Table S7) and the weight gain due to lipid uptake (Table S1).

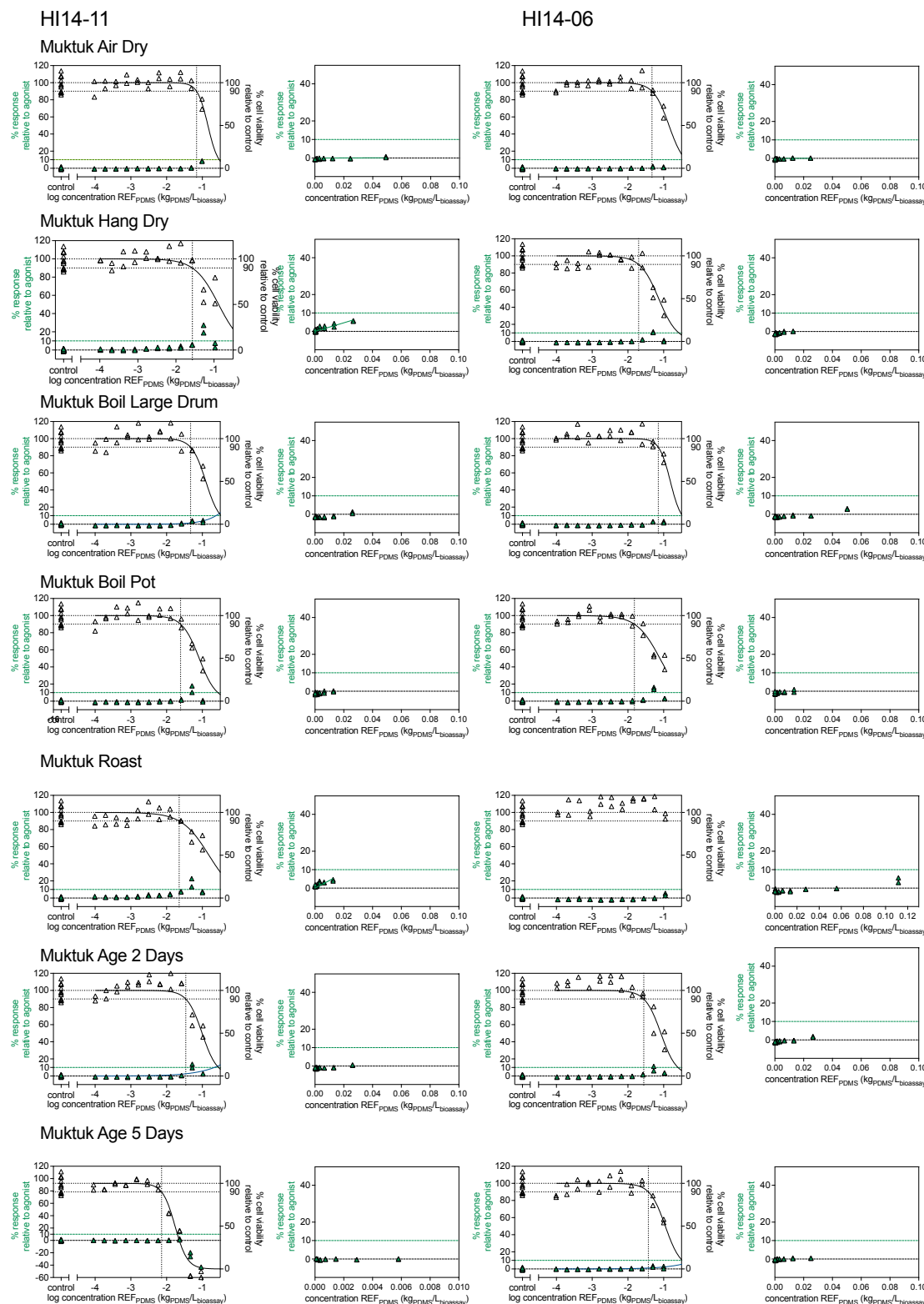


Figure S 10. Concentration-response curves for the Muktuk samples of whales HI-14-11 (left) and HI-14-06 (right) in the ER $\alpha$ -bla assay. For each sample, the left plot is on the log-concentration scale to determine the cytotoxicity. The vertical dotted line indicates the IC<sub>10</sub> for cytotoxicity. All % effect values above IC<sub>10</sub> concentrations or above 40% effect were excluded for the linear concentration response curves in each of the right plots. IC<sub>10</sub> values are in Table S3 and no activation of the estrogen receptor was detected.

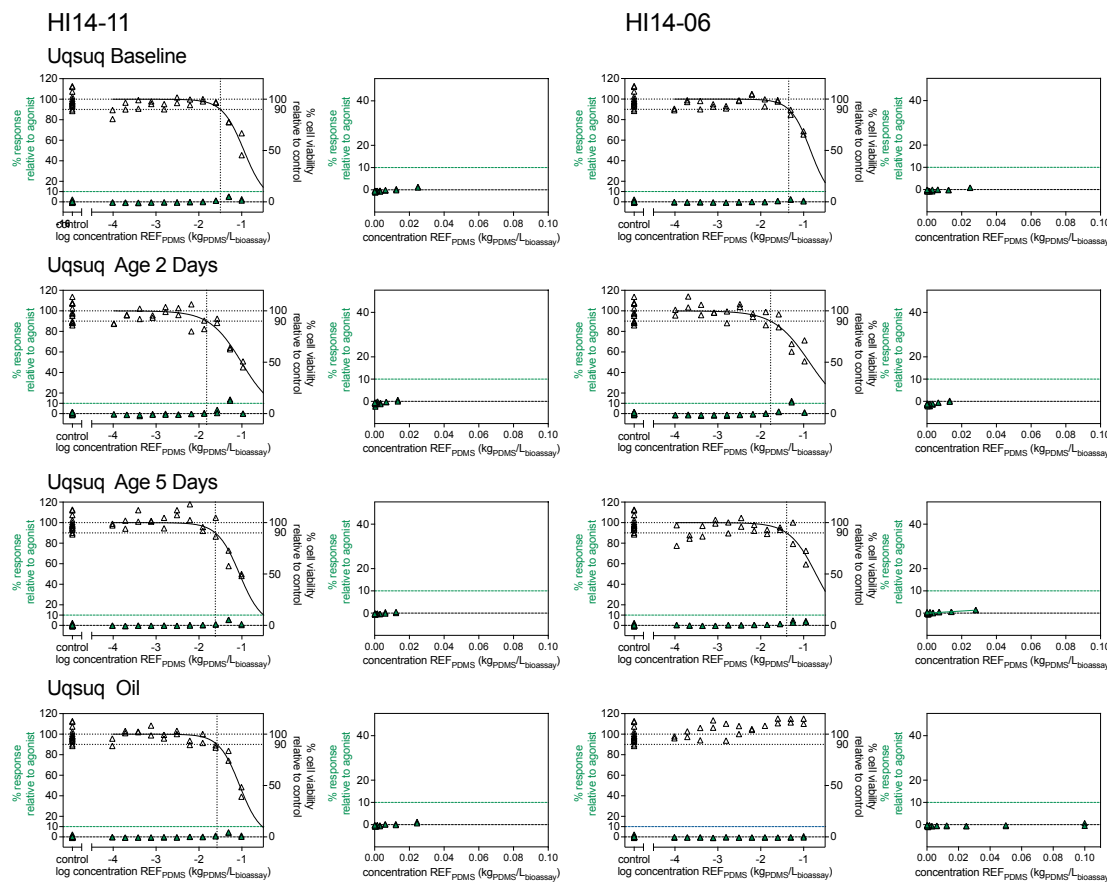


Figure S 11 Concentration-response curves for the Uqsuq samples of whales HI-14-11 (left) and HI-14-06 (right) in the ER $\alpha$ -bla assay. For each sample, the left plot is on the log-concentration scale to determine the cytotoxicity. The vertical dotted line indicates the IC<sub>10</sub> for cytotoxicity. All % effect values above IC<sub>10</sub> concentrations or above 40% effect were excluded for the linear concentration response curves in each of the right plots. IC<sub>10</sub> values are in Table S3 and no activation of the estrogen receptor was detected.

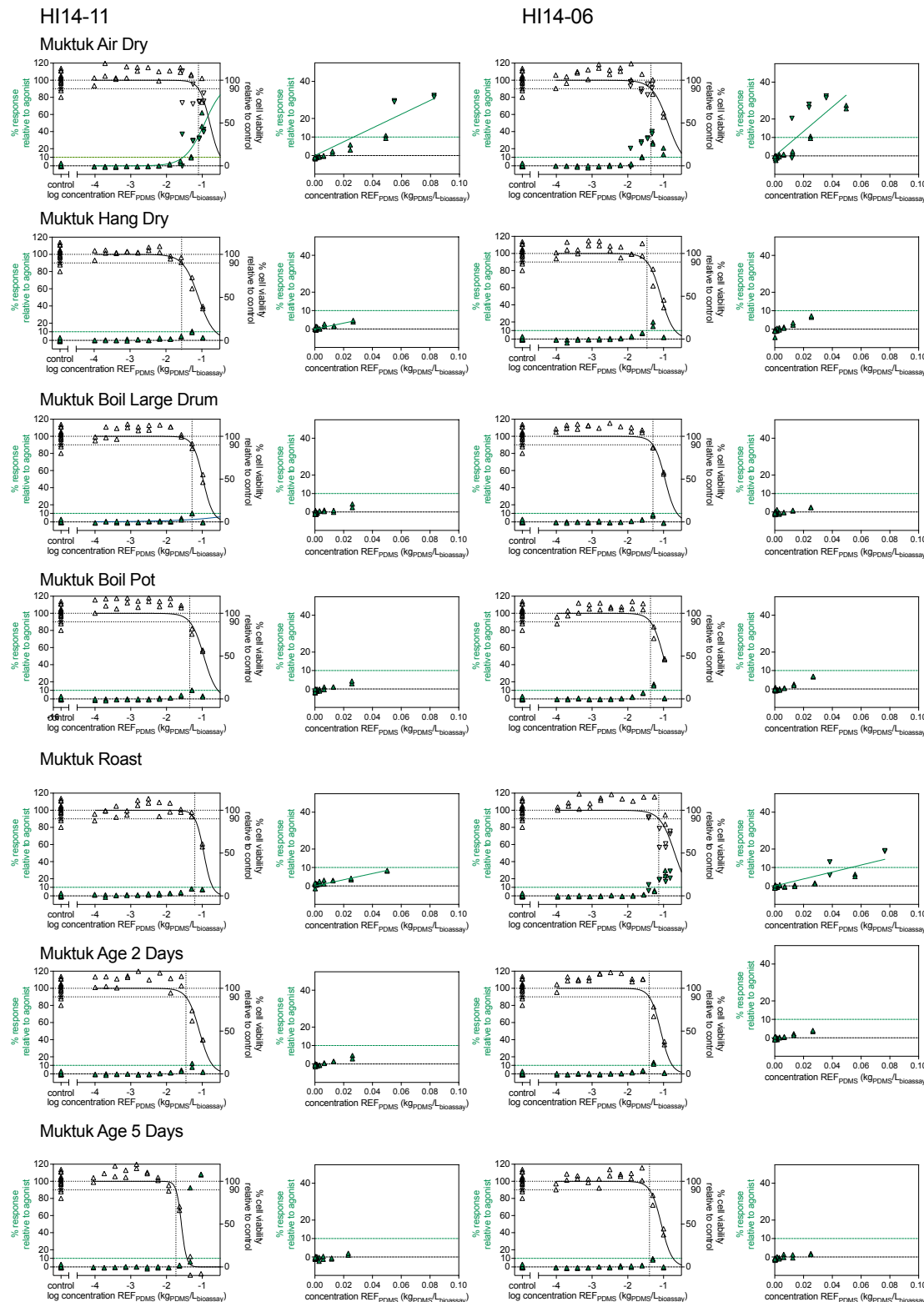


Figure S 12. Concentration-response curves for the Muktuk samples of whales HI-14-11 (left) and HI-14-06 (right) in the AR-bla assay. For each sample, the left plot is on the log-concentration scale to determine the cytotoxicity. The vertical dotted line indicates the IC<sub>10</sub> for cytotoxicity. All % effect values above IC<sub>10</sub> concentrations or above 40% effect were excluded for the linear concentration response curves in each of the right plots. IC<sub>10</sub> values are in Table S3 and no activation of the estrogen receptor was detected.

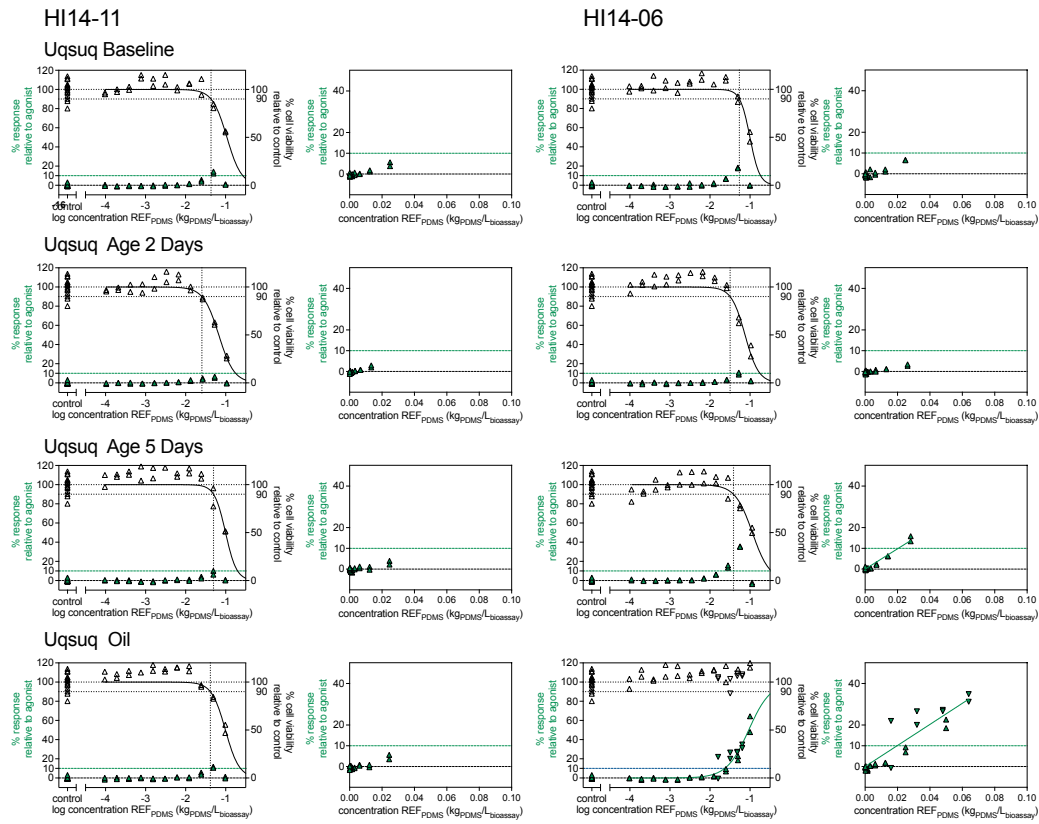


Figure S 13. Concentration-response curves for the Uqsuq samples of whales HI-14-11 (left) and HI-14-06 (right) in the AR-bla assay. For each sample, the left plot is on the log-concentration scale to determine the cytotoxicity. The vertical dotted line indicates the IC<sub>10</sub> for cytotoxicity. All % effect values above IC<sub>10</sub> concentrations or above 40% effect were excluded for the linear concentration response curves in each of the right plots. IC<sub>10</sub> values are in Table S3 and no activation of the estrogen receptor was detected.

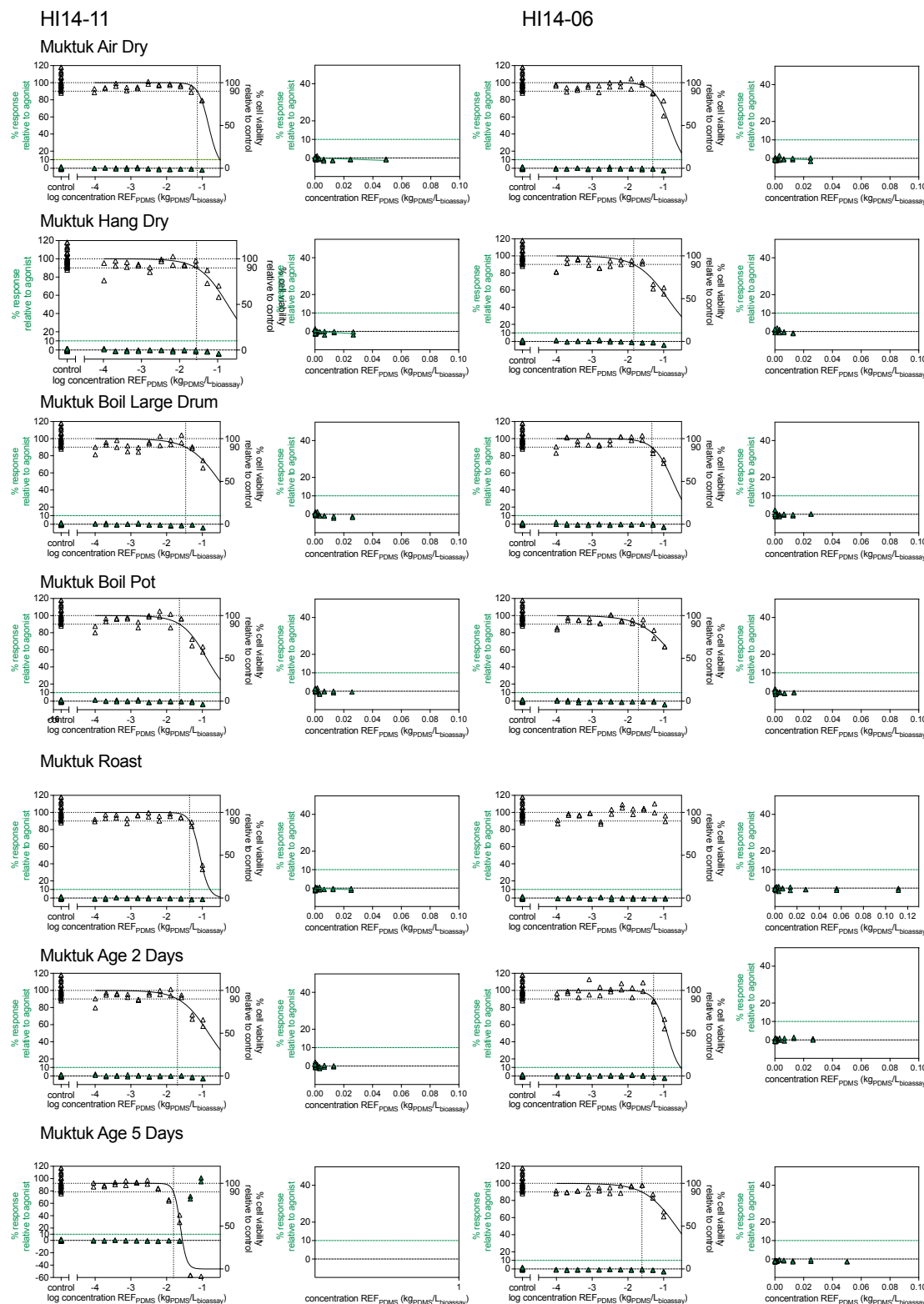


Figure S 14 Concentration-response curves for the Muktuk samples of whales HI-14-11 (left) and HI-14-06 (right) in the GR-bla assay. For each sample, the left plot is on the log-concentration scale to determine the cytotoxicity. The vertical dotted line indicates the IC<sub>10</sub> for cytotoxicity. All % effect values above IC<sub>10</sub> concentrations or above 40% effect were excluded for the linear concentration response curves in each of the right plots. IC<sub>10</sub> values are in Table S3 and no activation of the estrogen receptor was detected.

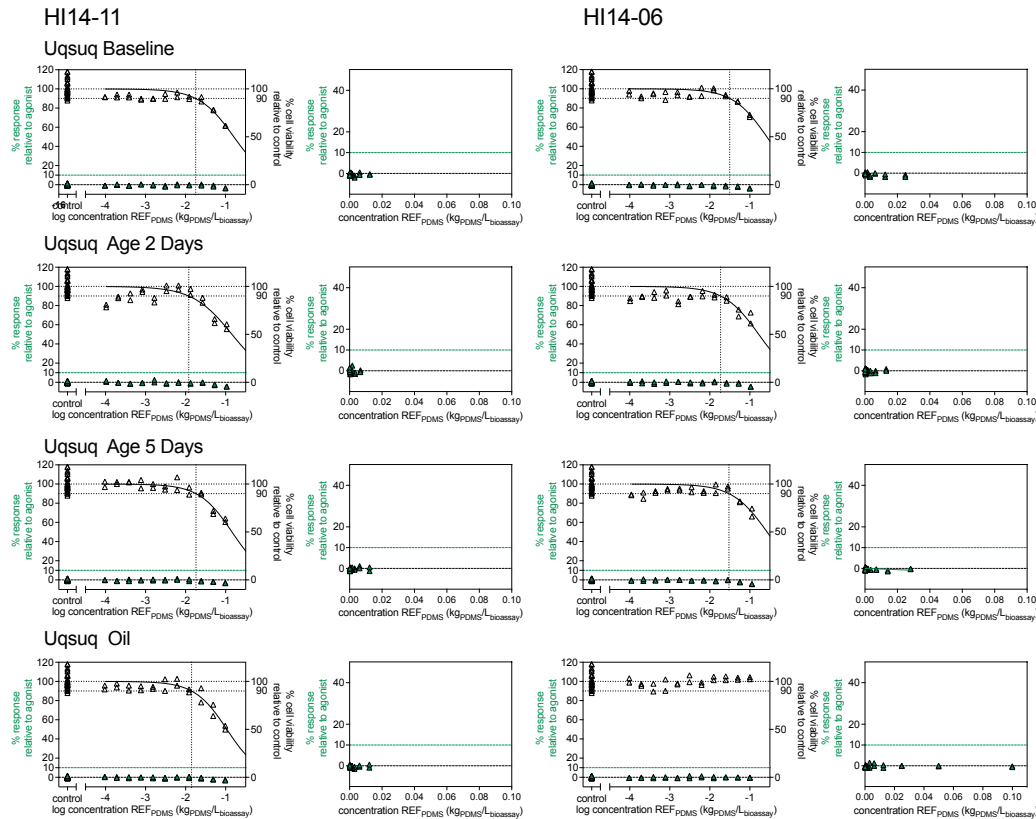


Figure S15 Concentration-response curves for the Uqsuq samples of whales HI-14-11 (left) and HI-14-06 (right) in the GR-bla assay. For each sample, the left plot is on the log-concentration scale to determine the cytotoxicity. The vertical dotted line indicates the  $IC_{10}$  for cytotoxicity. All % effect values above  $IC_{10}$  concentrations or above 40% effect were excluded for the linear concentration response curves in each of the right plots.  $IC_{10}$  values are in Table S3 and no activation of the estrogen receptor was detected.

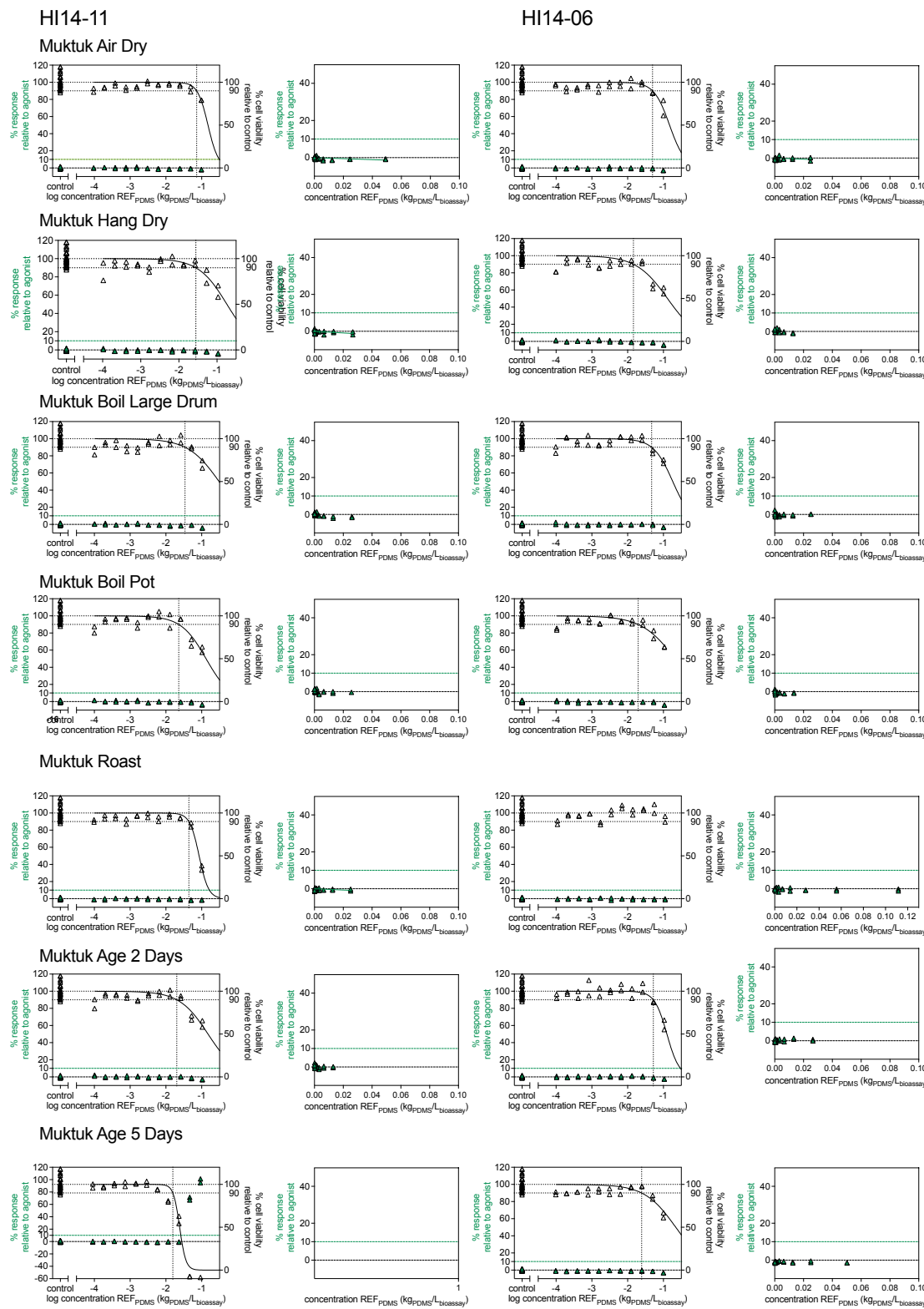


Figure S16. Concentration-response curves for the Muktuk samples of whales HI-14-11 (left) and HI-14-06 (right) in the PR-bla assay. For each sample, the left plot is on the log-concentration scale to determine the cytotoxicity. The vertical dotted line indicates the  $IC_{10}$  for cytotoxicity. All % effect values above  $IC_{10}$  concentrations or above 40% effect were excluded for the linear concentration response curves in each of the right plots.  $IC_{10}$  values are in Table S3 and no activation of the estrogen receptor was detected.

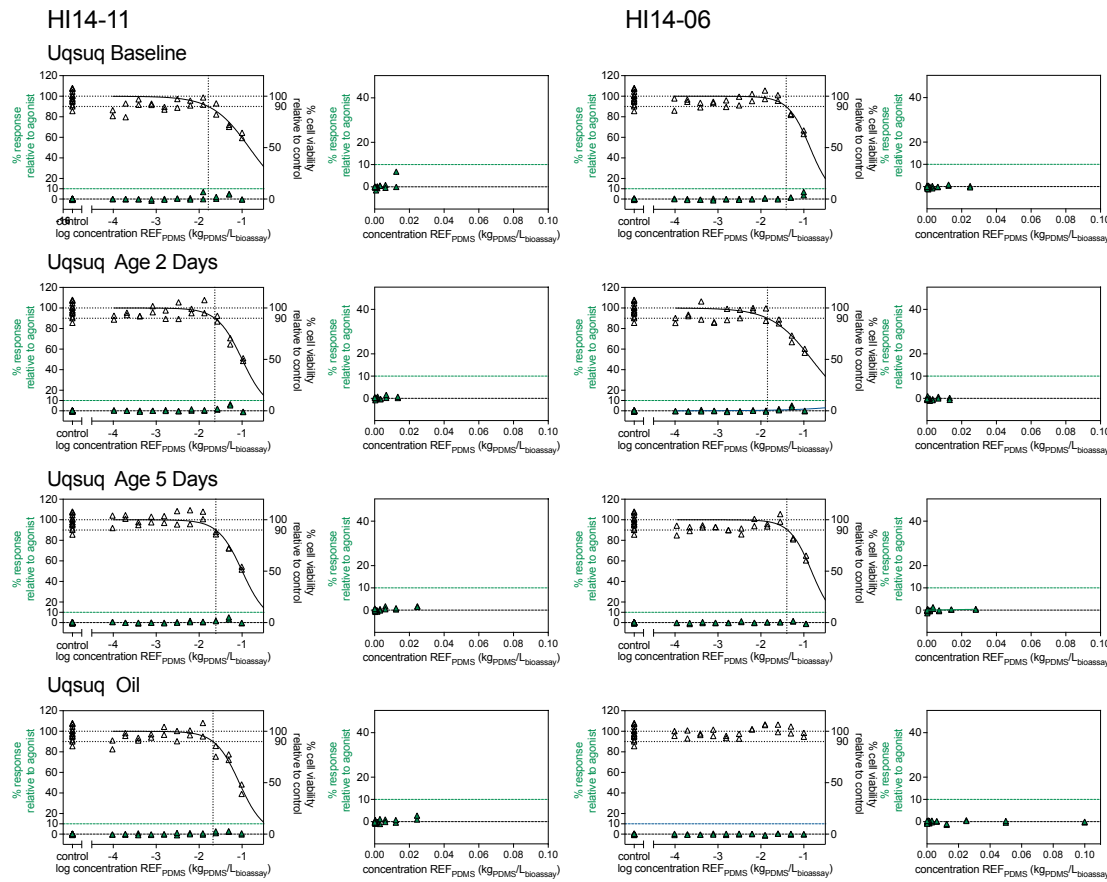


Figure S17. Concentration-response curves for the Uqsuq samples of whales HI-14-11 (left) and HI-14-06 (right) in the PR-bla assay. For each sample, the left plot is on the log-concentration scale to determine the cytotoxicity. The vertical dotted line indicates the  $IC_{10}$  for cytotoxicity. All % effect values above  $IC_{10}$  concentrations or above 40% effect were excluded for the linear concentration response curves in each of the right plots.  $IC_{10}$  values are in Table S3 and no activation of the estrogen receptor was detected.

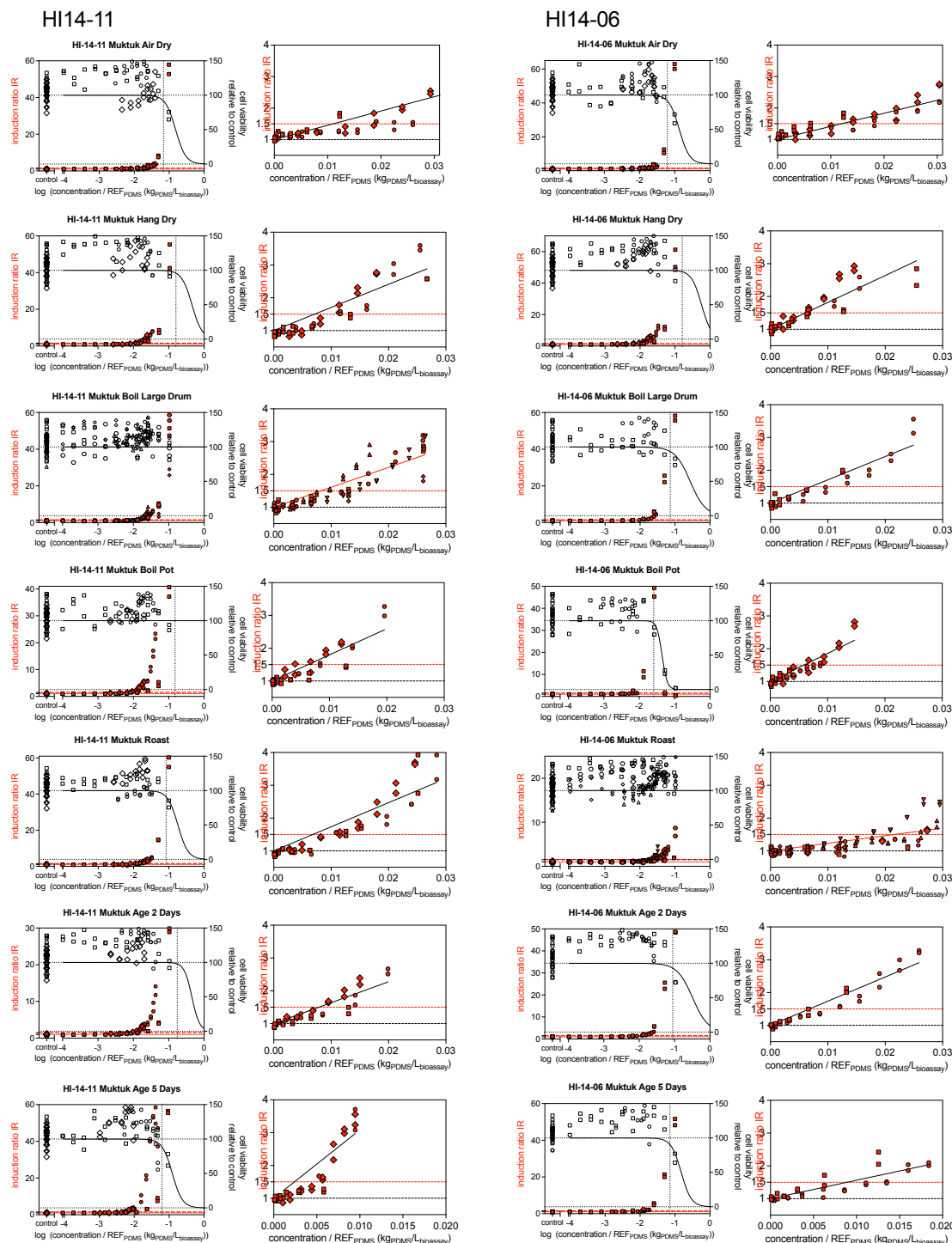


Figure S 18 .Concentration-response curves for the Muktuk samples of whales HI-14-11 (left) and HI-14-06 (right) in the AREc32 assay. For each sample, the left plot is on the log-concentration scale to determine the cytotoxicity. The vertical dotted line indicates the  $IC_{10}$  for cytotoxicity. All induction ratios (IR) values above  $IC_{10}$  concentrations or above IR 4 were excluded for the linear concentration response curves in each of the right plots. The  $EC_{IR1.5}$  is derived from the linear regression of the concentration versus IR. The red dotted line marks the IR 1.5.  $IC_{10}$  values are in Table S3 and  $EC_{IR1.5}$  values from the are in Table S4.

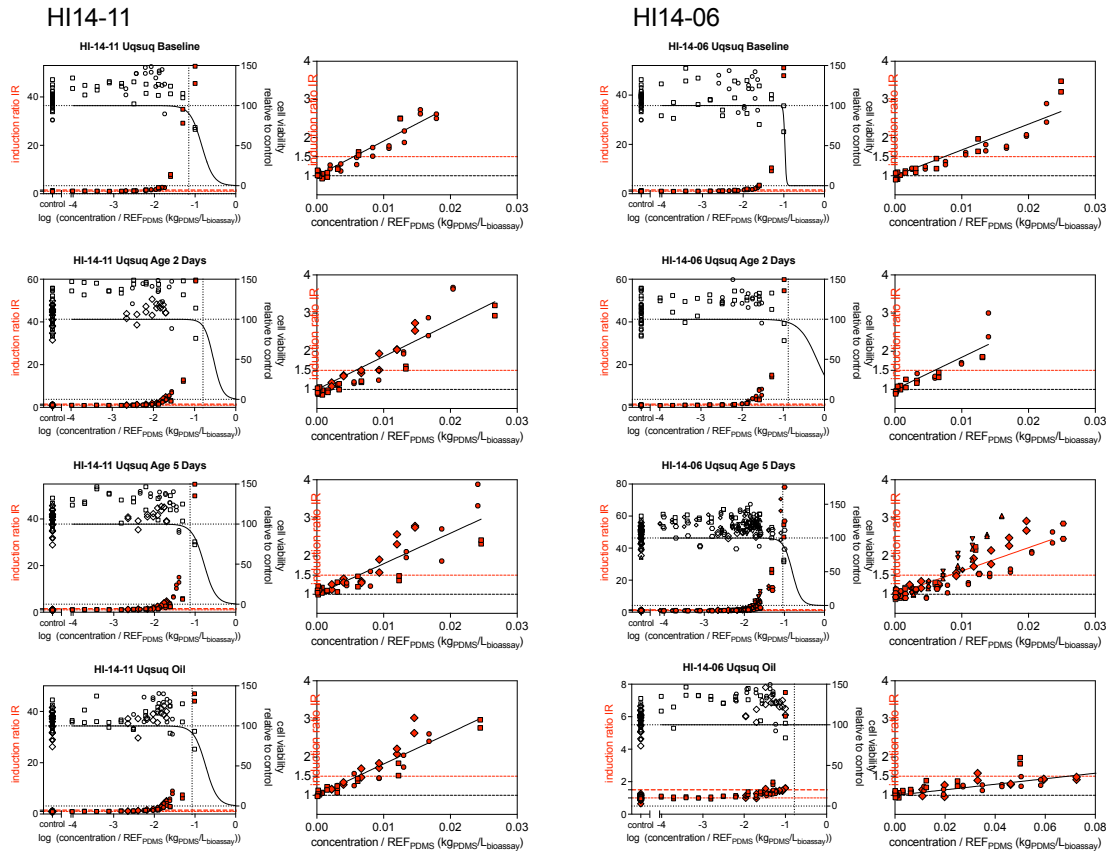


Figure S 19. Concentration-response curves for the Uqsuq samples of whales HI-14-11 (left) and HI-14-06 (right) in the AREc32 assay. For each sample, the left plot is on the log-concentration scale to determine the cytotoxicity. The vertical dotted line indicates the IC<sub>10</sub> for cytotoxicity. All induction ratios (IR) values above IC<sub>10</sub> concentrations or above IR 4 were excluded for the linear concentration response curves in each of the right plots. The EC<sub>IR1.5</sub> is derived from the linear regression of the concentration versus IR. The red dotted line marks the IR 1.5. IC<sub>10</sub> values are in Table S3 and EC<sub>IR1.5</sub> values from the are in Table S4.

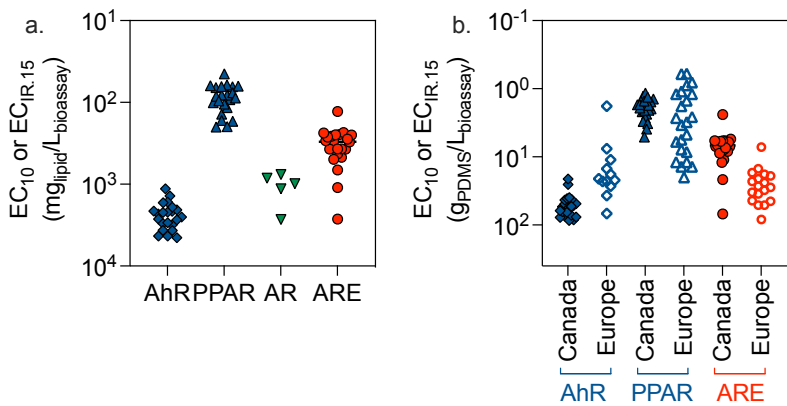


Figure S 20. (a) Comparison of effect concentrations EC<sub>10</sub> (AhR, PPAR, AR) and EC<sub>IR1.5</sub> (ARE) for the activation of reporter genes. Data in Table S4. (b) Comparison with data from literature (based on PDMS concentrations).<sup>2,3</sup>

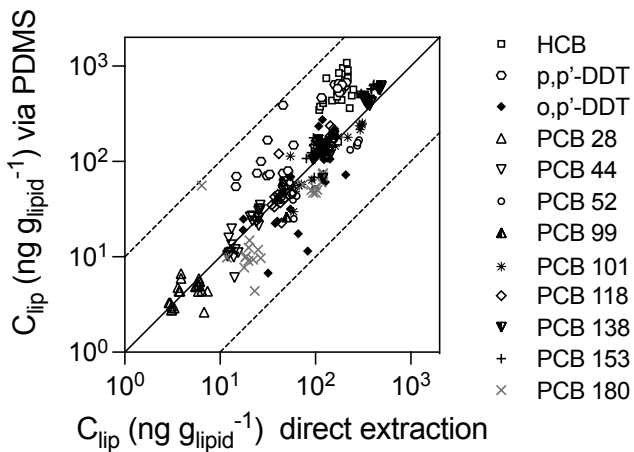


Figure S 21. Comparison of concentrations of analytes in lipids from direct extraction and via PDMS extraction. Data in Table S2 and S5.

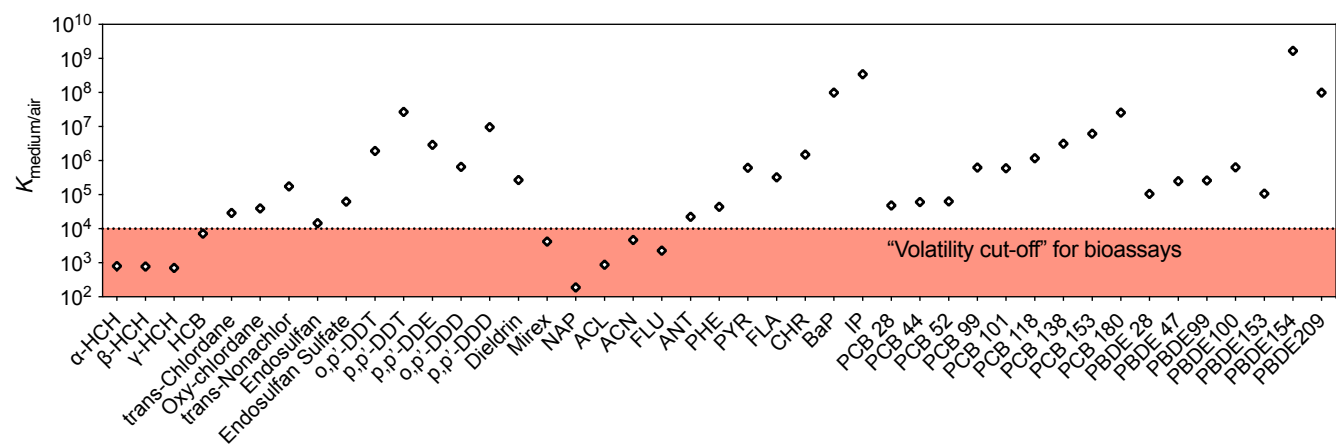


Figure S 22. Bioassay medium-air partition constants  $K_{medium/air}$  for all detected chemicals. The dotted line is the "volatility cutoff" of  $K_{medium/air} = 10^4$  and all chemicals with lower  $K_{medium/air}$  are expected to escape during the bioassay exposure.<sup>4</sup>

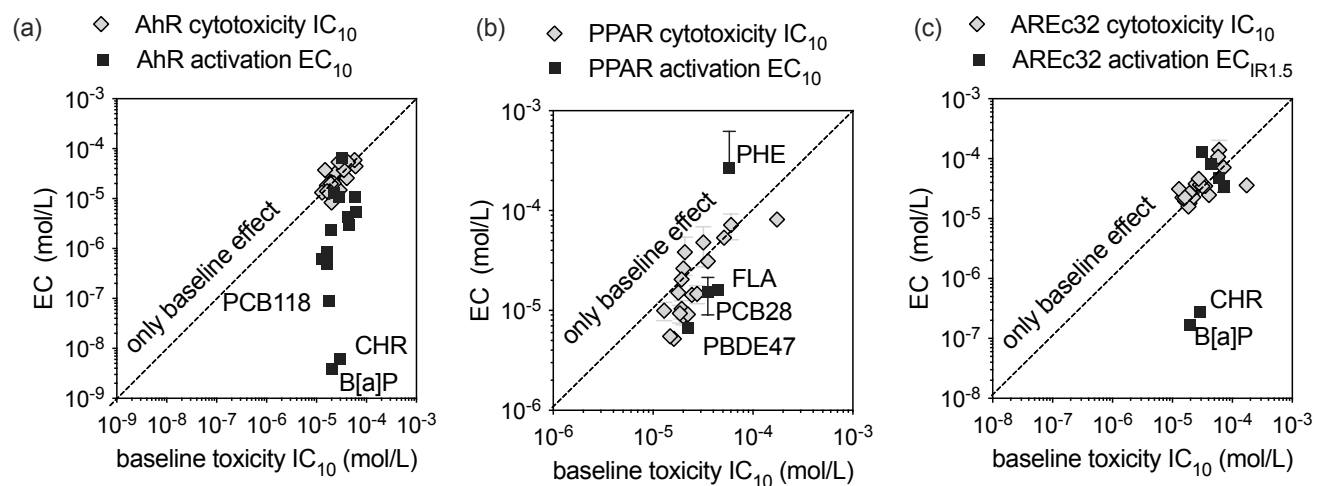


Figure S 23. Comparison between the predicted baseline toxicity  $IC_{10}$  calculated with the model of Lee et al.<sup>1</sup> and the measured cytotoxicity  $IC_{10}$  and response concentrations for the specific effects. Only chemicals below the 1:1 line show a specific effect, most chemicals are active but merely as baseline toxicants. Data from Table S6.

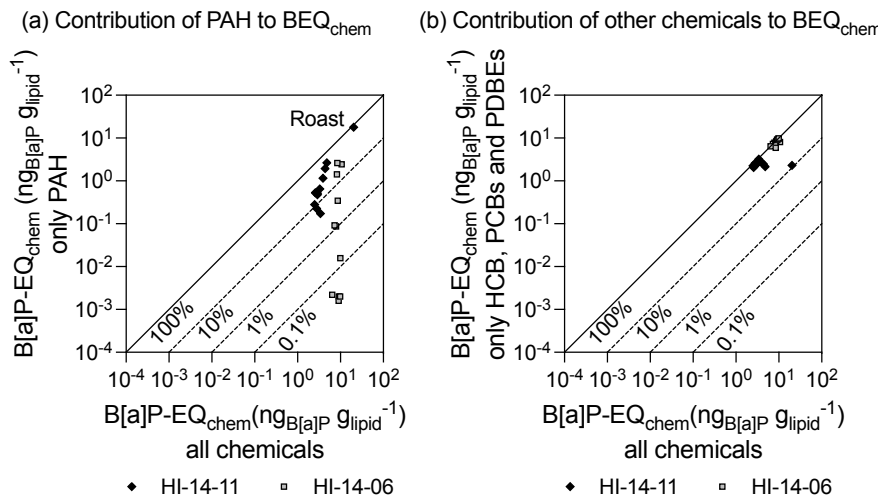


Figure S 24. Comparison between the bioanalytical equivalent concentrations predicted from the detected chemicals (BEQ<sub>chem</sub>) and the contribution to BEQ<sub>chem</sub> by (a) PAHs and (b) other chemicals in the AhR-CALUX. Data in Table S7.

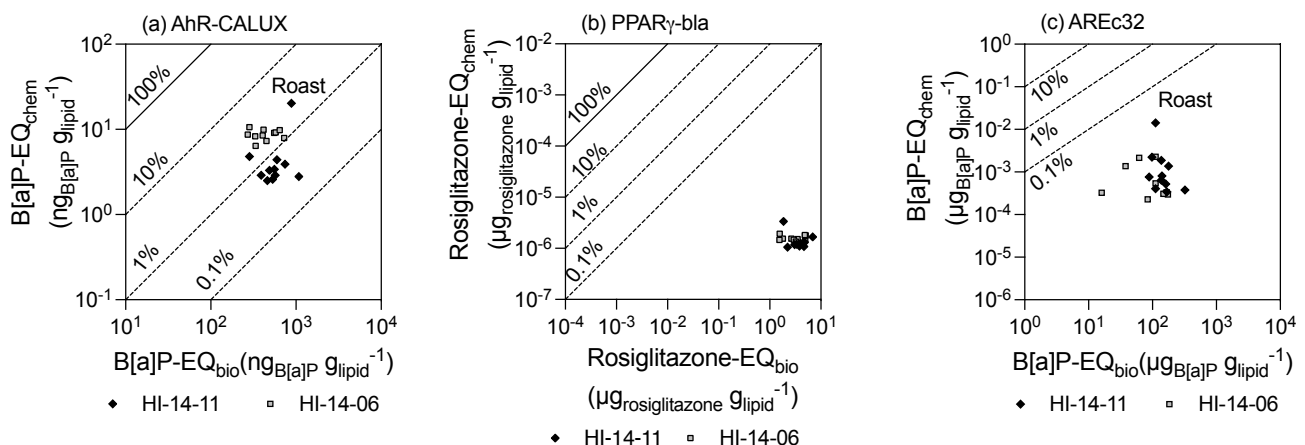


Figure S 25. Comparison between the bioanalytical equivalent concentrations as derived from the bioassays (BEQ<sub>bio</sub>) and as derived from the measured concentrations of the detected chemicals (BEQ<sub>chem</sub>) for (a) AhR-CALUX, (b) PPAR $\gamma$ -bla and (c) AREc32 Data in Table S7.

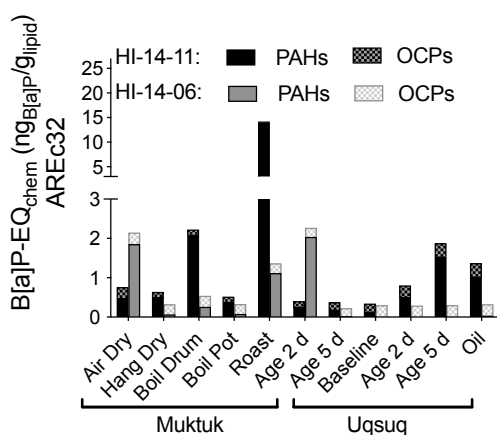


Figure S 26. Contribution of nonpersistent polycyclic aromatic hydrocarbons (PAHs) and persistent organochlorine pesticides (OCPs) to B[a]P-EQ<sub>chem</sub> in the AREc32 assay. Data in Table S7.

## References

1. J. Lee, G. Braun, L. Henneberger, M. König, R. Schlichting, S. Scholz and B. I. Escher, Critical Membrane Concentration and Mass-Balance Model to Identify Baseline Cytotoxicity of Hydrophobic and Ionizable Organic Chemicals in Mammalian Cell Lines, *Chem. Res. Toxicol.*, 2021, **34**, 2100-2109.
2. E. B. Reiter, B. I. Escher, E. Rojo-Nieto, H. Nolte, U. Siebert and A. Jahnke, Characterizing the marine mammal exposome by iceberg modeling, linking chemical analysis and in vitro bioassays, *Environmental Science: Processes & Impacts*, 2023, DOI: 10.1039/D3EM00033H.
3. E. B. Reiter, B. I. Escher , U. Siebert and A. Jahnke, Activation of the xenobiotic metabolism and oxidative stress response by mixtures of organic pollutants extracted with in-tissue passive sampling from liver, kidney, brain and blubber of marine mammals, *Environment International*, 2022, submitted.
4. B. I. Escher, L. Glauch, M. Konig, P. Mayer and R. Schlichting, Baseline Toxicity and Volatility Cutoff in Reporter Gene Assays Used for High-Throughput Screening, *Chem. Res. Toxicol.*, 2019, **32**, 1646-1655.